Redox Biology 17 (2018) 338–347

Contents lists available at ScienceDirect

Redox Biology

journal homepage: www.elsevier.com/locate/redox

Research Paper

Improvement of neuronal differentiation by carbon monoxide: Role of pentose phosphate pathway

Ana S. Almeida[a,b,c,1], Nuno L. Soares[a,1], Catarina O. Sequeira[a], Sofia A. Pereira[a], Ursula Sonnewald[d,2], Helena L.A. Vieira[a,c,*]

[a] CEDOC, Faculdade de Ciência Médicas/NOVA Medical School, Universidade Nova de Lisboa, 1169-056 Lisboa, Portugal
[b] Instituto de Tecnologia Química e Biológica (ITQB), Universidade Nova de Lisboa, Apartado 127, 2781-901 Oeiras, Portugal
[c] Instituto de Biologia Experimental e Tecnológica (iBET), Apartado 12, 2781-901 Oeiras, Portugal
[d] Norwegian University of Science and Technology, Norway

ARTICLE INFO

Keywords:
Carbon monoxide
Neuronal differentiation
Glycolysis
Pentose phosphate pathway
Glutathione

ABSTRACT

Over the last decades, the silent-killer carbon monoxide (CO) has been shown to also be an endogenous cytoprotective molecule able to inhibit cell death and modulate mitochondrial metabolism. Neuronal metabolism is mostly oxidative and neurons also use glucose for maintaining their anti-oxidant status by generation of reduced glutathione (GSH) via the pentose-phosphate pathway (PPP). It is established that neuronal differentiation depends on reactive oxygen species (ROS) generation and signalling, however there is a lack of information about modulation of the PPP during adult neurogenesis. Thus, the main goal of this study was to unravel the role of CO on cell metabolism during neuronal differentiation, particularly by targeting PPP flux and GSH levels as anti-oxidant system.

A human neuroblastoma SH-S5Y5 cell line was used, which differentiates into post-mitotic neurons by treatment with retinoic acid (RA), supplemented or not with CO-releasing molecule-A1 (CORM-A1). SH-SY5Y cell differentiation supplemented with CORM-A1 prompted an increase in neuronal yield production. It did, however, not alter glycolytic metabolism, but increased the PPP. In fact, CORM-A1 treatment stimulated (i) mRNA expression of 6-phosphogluconate dehydrogenase (PGDH) and transketolase (TKT), which are enzymes for oxidative and non-oxidative phases of the PPP, respectively and (ii) protein expression and activity of glucose 6-phosphate dehydrogenase (G6PD) the rate-limiting enzyme of the PPP. Likewise, whenever G6PD was knocked-down CO-induced improvement on neuronal differentiation was reverted, while pharmacological inhibition of GSH synthesis did not change CO's effect on the improvement of neuronal differentiation. Both results indicate the key role of PPP in CO-modulation of neuronal differentiation. Furthermore, at the end of SH-SY5Y neuronal differentiation process, CORM-A1 supplementation increased the ratio of reduced and oxidized glutathione (GSH/GSSG) without alteration of GSH metabolism. These data corroborate with PPP stimulation. In conclusion, CO improves neuronal differentiation of SH-S5Y5 cells by stimulating the PPP and modulating the GSH system.

1. Introduction

Stem cell fate can be regulated by various factors, namely cellular energy metabolism, which is capable of modulating stem cell decision between self-renewing or differentiation [1–3]. Thus, manipulation of cell metabolism can be a key tool for neurogenesis modulation. In fact, stimulation of endogenous neurogenesis can be particularly important for replacement of impaired neurons in central nervous system (CNS), in future potential applications against neurodegenerative diseases including ischemic stroke and psychiatric disorders.

Abbreviations: G6PD, glucose 6-phosphate dehydrogenase; CNS, central nervous system; CO, carbon monoxide; CORM-A1, Carbon monoxide-releasing molecule A1; COX, cytochrome c oxidase; DMEM/F12, Dulbecco's minimum essential medium with nutrient mixture F12; FBS, foetal bovine serum; Cys, cysteine; CysGly, cysteine-glycine; GC-MS, gas chromatography coupled with mass spectrometry analysis; G6PD, glucose 6-phosphate dehydrogenase; GSH, reduced glutathione; GSSG, oxidized glutathione; HO-1, Haem-oxygenase 1; HPLC, High performance liquid chromatography; LDH, lactate dehydrogenase; NAC, N-acetylcysteine; NSC, neural stem cell; PBS, phosphate buffered saline; PDH, pyruvate dehydrogenase; Pen/Strep, penicillin/streptomycin solution; PGD, phosphogluconate dehydrogenase; PPP, Pentose phosphate pathway; RA, retinoic acid; ROS, reactive oxygen species; RT-Q-PCR, Reverse transcriptase quantitative polymerase chain reaction; R.T., room temperature; TCA, Tricarboxilic acid cycle; TKT, transketolase; UV, ultra violet radiation

* Corresponding author at: Chronic Diseases Research Center (CEDOC), NOVA Medical School / Faculdade de Ciências Médicas, Universidade Nova de Lisboa, Campo dos Mártires da Pátria 130, 1169-056 Lisboa, Portugal.
E-mail address: helena.vieira@nms.unl.pt (H.L.A. Vieira).
[1] These authors equally contributed to this work.
[2] Formerly.

https://doi.org/10.1016/j.redox.2018.05.004
Received 3 April 2018; Received in revised form 24 April 2018; Accepted 10 May 2018
Available online 15 May 2018

The Pentose Phosphate Pathway (PPP) is an important route of glucose oxidation, divided into two branches, the oxidative and non-oxidative phase, where, by multiple reactions, sugar phosphates are interconverted. The oxidative phase of PPP is linked to glycolysis at the level of glucose-6-phosphate and catalyses its conversion into ribulose-5-phosphate and CO_2. Also in this phase, $NADP^+$ is reduced into NADPH, the major reducing compound, which is required for re-generation of reduced glutathione (GSH). On the other hand, the non-oxidative phase converts pentose phosphates into phosphorylated aldoses and ketones. This branch is linked to glycolysis by their common intermediates glyceraldehyde-3-phosphate and fructose-6-phosphate and it also produces ribose-5-phosphates, which are precursors for nucleotide synthesis [4,5]. The activity of this non-oxidative phase of PPP supports cellular proliferation during neurogenesis by the production of building blocks [6]. In addition, during neuronal differentiation process, there is an enhancement of mitochondrial and oxidative cell metabolism [3,7], which, in turn, increases ROS production. Thus, one can speculate oxidative phase of PPP can be critical during neuronal differentiation for reinforcing cellular anti-oxidant defence. Indeed, PPP generates reducing molecules NADPH, which facilitates recycling of oxidized GSSG into reduced GSH, the first line of cell antioxidant defence [8].

CO is mostly known as a silent-killer due to its great affinity to haem-proteins, such as haemoglobin or cytochrome c oxidase (COX). Thus, high levels of CO can compromise systemic oxygen delivery or cellular mitochondrial function, promoting high levels of intoxication and even death. Nevertheless, CO is an endogenously produced gasotransmitter generated by the cleavage of haem group via the enzymatic activity of haem-oxygenase (HO) [9]. HO is a stress-related enzyme, whose expression or activity increases in response to several stressful stimuli including oxidative stress, hypoxia, hyperoxia, hyperthermia, inflammation, UV and misfolded protein response [9–11]. Furthermore, it has been demonstrated that low levels of exogenous CO promote cytoprotection, limit inflammation, prevent cell death and improve neuronal differentiation [9,10,12–18]. The molecular mechanisms underlying CO-induced cytoprotection are associated with improvement of mitochondrial function and are dependent on generation of low amounts of ROS, as signalling molecules [12,19–22]. Likewise, low concentrations of CO promote mitochondrial biogenesis [23,24], increase COX activity [13,25–28], improve oxidative metabolism [23,29] and induce mild mitochondrial uncoupling that protects mitochondria from oxidative stress [30,31]. For further reading, there are reviews [23,32,33]. Because of the great potential use of CO as a therapeutic gas, several strategies to deliver CO under biological context have been developed. CO-releasing molecules (CORM) are small organic or organometallic molecules able to release CO under a more physiologically relevant way than CO gas applications [34]. CORM-A1 (carbon-monoxide releasing molecule A1) is a boron-based molecule that has been often studied because it slowly releases CO under a controlled manner. CO-releasing is dependent on temperature and pH, with optimal release at pH of 7.4 and 37 °C and it presents a half-life of approximately 21 min to transfer CO to myoglobin in vitro [35,36].

Recently, it has been demonstrated that CO promotes neuronal differentiation [16] and increases dopaminergic differentiation [18]. The underlying molecular mechanisms of neuronal differentiation involve CO-induced improvement of mitochondrial metabolism [17]. Likewise, CO modulates cellular GSH levels in astrocytes [12] and GSSG/GSH recycling is dependent on PPP. Thus, it is hypothesized that CO can stimulate PPP flux, which in turn, facilitates the cellular machinery rearrangement needed during neuronal differentiation. For assessing PPP modulation by CO, a human neuroblastoma SH-S5Y5 cell line was used as cell model. This is a simple model to study neuronal differentiation process [37], allowing the assessment of the associated cellular mechanisms. SH-SY5Y cells are derived from neural crest [38,39] and present the ability to differentiate into neuron-like cells that fulfil the morphological, biochemical and functional neuronal criteria [37,39,40], constituting a valuable model also for neuronal toxicity studies [41–44].

The main goal of this study was to assess the metabolic regulation of neuronal differentiation achieved by CO, in particular, the role of PPP. CORM-A1 supplementation increased the yield of neuronal production following SH-SY5Y neuronal differentiation, along with an increase of ROS generation, PPP flux and a change in GSH availability. Likewise, whenever the limiting PPP enzyme glucose 6-phosphate dehydrogenase (G6PD) was knocked down, the CO-induced increase of neuronal yield was reverted, while pharmacological inhibition of GSH synthesis had no effect on neuronal differentiation. In conclusion, in the SH-SY5Y model of adult neurogenesis, CO improves neuronal differentiation in a PPP dependent manner.

2. Material and methods

2.1. Materials

All chemicals were of analytical grade and were obtained from Sigma unless stated otherwise. Plastic tissue culture dishes were from Sarstedt (Germany); foetal bovine serum, penicillin/streptomycin solution, and Dulbecco's minimum essential medium (high glucose, L-glutamine and pyruvate) were obtained from Invitrogen (United Kingdom).

The mass spectrometry derivatization reagents MTBSTFA (*N*-methyl-*N*-(*tert*-butyldimethylsilyl) trifluoroacetamide), MSTFA (*n*-methyl-*n*-(trimethylsilyl) trifluoroacetamide) and the t-BDMS-Cl (tert-butyldimethylchlorosilane) were purchased from Regis Technologies, Inc. (Morton Grove, IL, USA). All other chemicals were of the purest grade available from regular commercial sources.

For liquid chromatography, the reduction reagent TCEP (Tris(2-carboxyethyl)phosphine hydrochloride) and derivatization reagent SBD-F (7-fluorobenzofurazan-4-sulfonic acid ammonium salt) and the standards used, namely Cys (cysteine), CysGly (cysteinylglycine), GluCys (glutamylcysteine) and GSH (γ-glutamyl-cysteinylglycine) were purchased from Sigma-Aldrich.

2.2. SH-SY5Y human neuroblastoma cell line

2.2.1. Maintenance of undifferentiated cells

The SH-SY5Y cell line was cultured in DMEM/F-12 supplemented with 10% (v/v) FBS and 2% (v/v) Pen/Strep (growth medium). Cells were maintained in a humidified atmosphere of 5% (v/v) CO_2 at 37 °C. Undifferentiated cells were grown in 75 cm^2 T-flasks and sub-cultured with fresh growth medium, whenever cell confluence achieved (about 80–90% cell confluence). Cells were detached by trypsinization at room temperature (R.T.) and slight shaking and hitting to drain down cells with trypsin and resuspended in growth medium in a 1:4 cell passage. Growth medium was changed twice a week.

2.2.2. Neuronal differentiation protocol

Following trypsinization and resuspension in growth medium, cells were plated on 75 cm^2 T-flasks in a 1:2 cell passage. Neuronal differentiation was induced 24 h after plating undifferentiated cells to ensure settle and attachment to flask surface and attain appropriate density, approximately about 50% cell confluence in all 75 cm^2 T-flasks.

Neuronal differentiation was stimulated using DMEM/F-12 medium, reduced serum to 1% (v/v) FBS, 2% (v/v) Pen/Strep and supplemented with 10 μM of *all-trans* RA (differentiation medium). CO effect was studied by using the same composition of differentiation medium supplemented with 25 μM CORM-A1. Whenever necessary, buthionine sulfoximine (BSO) at 50 μM was added in differentiation medium for preventing GSH synthesis. Differentiation medium was replaced twice (day 1 and day 4) during 7 days of treatment (Fig. 1A). On day 7, cells were collected for analysis.

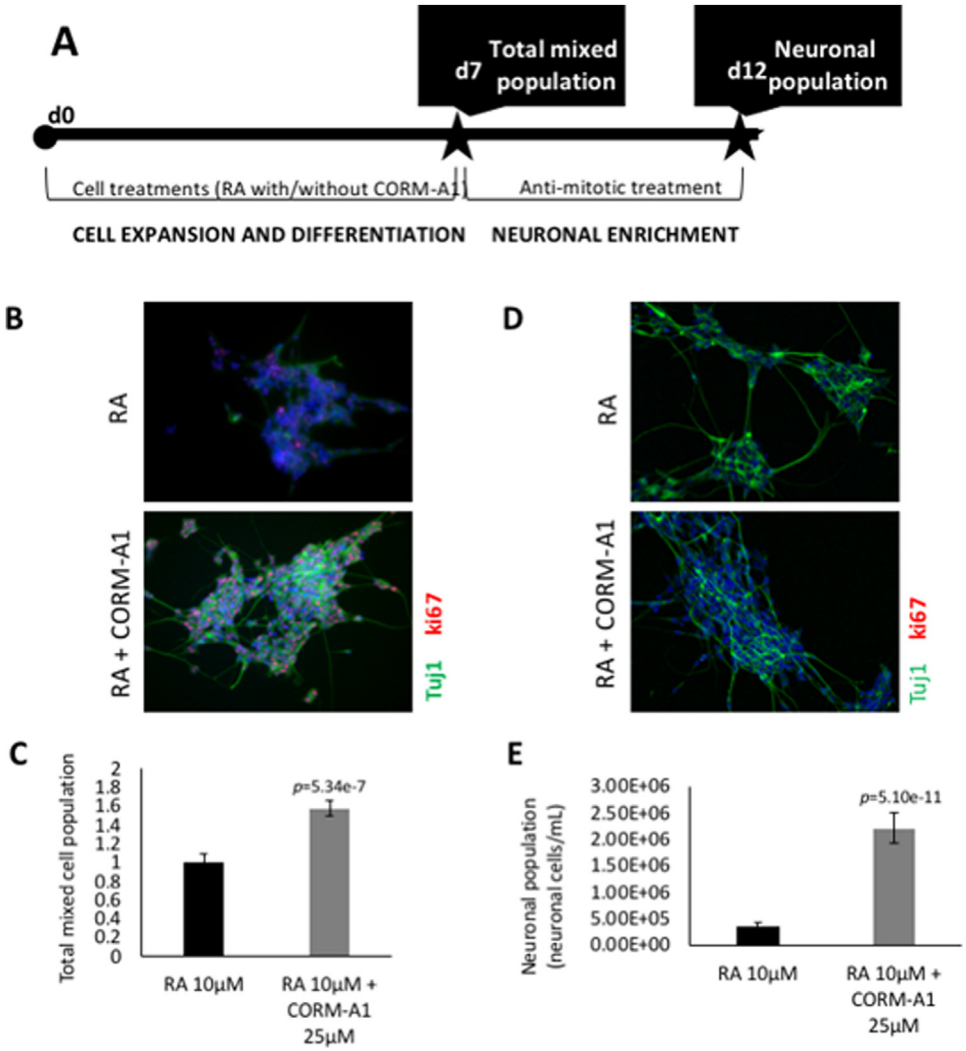

Fig. 1. SH-SY5Y neuronal differentiation procedure and CORM-A1 improves neuronal differentiation yield. (A) SH-SY5Y cells were induced to differentiate during 7 days (d7) with 10 µM of RA treatment with or without 25 µM of CORM-A1, subjected to a differentiation medium exchange at day 4. After 7 days of differentiation (d7), a mixed population of undifferentiated cells and post-mitotic neurons was obtained. In order to obtain an enriched neuronal population, cultures are treated with anti-mitotic compounds for 5 days (d12). (B, C) Characterization of SH-SY5Y cells by immunocytochemistry (green staining: Tuj1; blue staining: DAPI; red staining: ki67; magnification 100 ×); (D) nuclei counting of total mixed cell population, using RA at 10 µM as reference and (E) nuclei count of neuronal enriched cell population. After 7 days of differentiation (B, D) and after anti-mitotic treatment during 5 days (C, E). The used statistical analysis was unpaired two-tailored *t-test*.

2.2.3. Neuronal enrichment

After the day 7 of differentiation, cells were replated at lower density to disperse cell culture for neuronal enrichment. The culture medium was exchanged on the following day, with fresh growth medium supplemented with mitosis inhibitors: 1 µM cytosine arabinoside, 10 µM floxuridine and 10 µM uridine for neuronal enrichment. Growth medium supplemented with mitosis inhibitors was replaced after 2 days. On the day 5 of neuronal enrichment, enriched cultures were collected for different analysis. The used protocol is schematically represented in Fig. 1A.

2.3. Carbon monoxide-releasing molecule A1 (CORM-A1)

The solution of CORM-A1 was prepared in milli-Q water with a final concentration of 5 mM. Then, the solution was filtrated with 0.2 µM filter and stored at − 20 °C. For each use, an aliquot was thawed and immediately used.

2.4. Preparation of inactivated CORM-A1

CO-depleted inactive form (iCORM-A1) was generated to be used as a negative control by initially dissolving CORM-A1 in 0.1 M HCl and then bubbling pure N_2 through the solution for 10 min in order to remove all residual CO gas [36]. The solution of iCORM-A1 was adjusted to pH 7.4, filtrated using a 0.2 µM filter and stored at − 20 °C. For each use, an aliquot was thawed and immediately used.

2.5. Cell counting and viability

Cell cultures were visualized using an inverted microscope with phase contrast (DM IRB, Leica, Germany). Total cell number was determined by counting cell nuclei using a Fuchs-Rosenthal haemacytometer, after digestion with 0.1 M citric acid/1% Triton X-100 (wt/wt)/0.1% crystal violet (wt/v).

2.6. Quantitative-Polymerase chain reaction (Q-PCR)

Genomic DNA was extracted from cells after differentiation using the High Pure PCR Template preparation kit (Roche Diagnostics, Mannheim, Germany). PCR was performed using specific forward and reverse primers designed for the mitochondrial COXII gene (5'-ACAG ACGAGGTCAACGATCC-3' and 5'-AGATTAGTCCGCCGTAGTCG-3') and for the GAPDH gene (5'-GCATCCTGGGCTACACTGAG-3' and 5'-GTCA AAGGTGGAGGAGTGGG-3'), respectively. Fast Start DNA Master plus SYBR Green I (Roche Diagnostics) was used with the experimental run protocol: denaturation program was 95 °C for 10 min, followed by 45 cycles of 95 °C for 15'', 60 °C for 6'' and 72 °C for 20''.

For evaluation of gene expression, mRNA was extracted from NT2 and SH-SY5Y cells using High Pure RNA isolation kit (Roche Diagnostics), and cDNA synthesis was performed using the Transcriptor High Fidelity cDNA synthesis kit (Roche Diagnostics). PCR was performed using specific forward and reverse primers designed for the phosphogluconate dehydrogenase gene (5'-ACCAGCAGACAATGCAC

GTA-3' and 5'- AGGGATGAAGACAGCCACAC-3'), transketolase gene (5'- CATGCCAGTGACCGCATCAT-3' and 5'- ATGCGAATCTGGTCAAA GGC-3'), pyruvate dehydrogenase gene (5′-AGGGTGGTTTCTATCTGTC TTGT-3′ and 5′-TCATGCTTCTTTTATCCTCTTGCT-3′), lactate dehydrogenase gene (5′-GGCTATTCTTGGGCAACCCT-3′ and 5′-TGGAAGTG GTACCAATACAACTCA-3′) and RPL22 gene (5'-CACGAAGGAGGAGTG ACTGG-3' and 5'-TGTGGCACACCACTGACATT-3'), respectively. Fast Start DNA Master Plus SYBR Green I (Roche Diagnostics) was used with the experimental run protocol: denaturation program was 95 °C for 10 min, followed by 45 cycles of 95 °C for 10", 60 °C for 10" and 72 °C for 10".

2.7. Lactate/glucose ratio

Total glucose and lactate concentrations in the culture supernatant were determined by automated enzymatic assays (YSI 7100 Multiparameter Bioanalytical System; Dayton, OH). The rate of lactate production and glucose consumption was obtained by linear regression of the metabolites concentrations.

2.8. Gas chromatography-mass spectrometry (GC-MS)

For analysis of ^{13}C percent enrichment in intracellular metabolites cell extracts were lyophilized and resuspended in 0.01 M HCl followed by pH adjustment to pH < 2 with 6 M HCl. Samples were dried under atmospheric air (50 °C), and metabolites were derivatized with MTBSTFA in the presence of 1% *t*-BDMS-Cl, see references [45,46] for further details. The samples were analysed on an Agilent 6890 gas chromatograph connected to an Agilent 5975B mass spectrometer (Agilent Technologies, Palo Alto, CA, USA). The parent ion (M) and atom percent excess ^{13}C atoms (M+1, M+2, etc) values for 3PG, PEP, alanine, aspartate, lactate, citrate and glutamate were calculated from GC-MS data using MassHunter software supplied by Agilent (Agilent Technologies, Palo Alto, CA, USA) and correcting for the naturally abundant ^{13}C by using non-enriched standards [47].

2.9. Immunofluorescence microscopy

SH-SY5Y cells were plated at a density of 2×10^6 cells/well in 24-well plates coated with Poly-D-lysine in 0.15 M sodium borate buffer solution pH 8.4. Cells were fixed with 4% (v/v) PFA and 4% (w/v) sucrose solution, for 20 min at R.T., and then permeabilized with 0.3% (v/v) Triton X-100 solution, for 15 min at R.T. Later, cells were incubated 2 h at R.T. with primary antibody: Tuj1 (Sigma-Aldrich, T8660) and ki67 (Millipore, AB9260), following incubation for 1 h at R.T. with secondary antibody: AlexaFluor 488 anti-mouse (A11001) or AlexaFluor 594 anti-rabbit (A11012). Primary and secondary antibodies were dilute in 1% (v/v) BSA and 0.1% (v/v) Triton X-100 solution. Cultures were mounted on Prolong mounting media (with DAPI - Invitrogen) and images were captured with Zeiss Axiovert 40 CFL microscope. All solutions were prepared in PBS (1 ×). Washes with PBS (1 ×) solution were performed between each step.

2.10. Immunoblotting

SH-SY5Y cell samples were collected with lysis buffer, which consisted of 50 mM Tris-HCl, pH 6.8, 10% glycerol (v/v) and 2% SDS (w/v). Protein concentration was determined using the Pierce BCA Protein Assay Kit and was measured at 540 nm. Total protein extract (30 µg) was mixed with 10 mM DTT, 10% (v/v) and 0.005% (w/v) bromophenol blue, loaded into 12% polyacrylamide gels and electrically transferred to a nitrocellulose membrane (HybondTM-C extra, Amersham Biosciences). The membranes were blocked with 5% BSA in TBS with 0.1% Tween-20 (TBS-T) and subsequently incubated with primary antibodies in 5% BSA in TBS-T. Antibodies were against G6PD (Santa Cruz Biotechnology) used at 1/200 dilution and against α-actin (A4700; Sigma- Aldrich) used at 1/1000 dilution for 2 h at R.T. Blots were developed using the ECL (BioRad) detection system after incubation with horseradish peroxidase (HRP)-labelled anti-mouse or anti-rabbit IgG antibody (Amersham Bioscience), 1/5000, 1 h of incubation at R.T. These experiments have been repeated three times.

2.11. G6PD siRNA transfection

G6PD protein expression was silenced by G6PD coding siRNA transfection according to the instructions of the manufacturer (Santa Cruz Biotech). SH-SY5Y cells at 40–60% confluence were transfected using Lipofectamine™ RNAiMAX and 10 pmol of G6PD siRNA (Santa Cruz Biotech) in Opti-MEM medium® (Invitrogen). Culture medium was gently mixed at room temperature, allowing the formation of liposomes. Cells were subsequently transfected in the absence of antibiotics. In the next 27 h and 48 h, the efficiency of transfection was assessed by Western Blot assay.

2.12. G6PD activity

G6PD activity was measured by a commercially available kit from Sigma-Aldrich (Glucose-6-phosphate dehydrogenase Activity Assay Kit MAK015), based on colorimetry and manufactor's instructions were followed.

2.13. High Performance Liquid Chromatography (HPLC)

An HPLC with fluorescence detection was used to quantify the *glutathiomic* profile: the fraction of GSH in its free form and bound to proteins; glutathione in the reduced (GSH) and oxidized form (GSSG) in order to obtain GSH/GSSG ratio; as well as the GSH precursor cysteine (Cys) and glutamylcysteine (CysGlu); and the GSH degradation product cysteinylglicine (CysGly). Following 7 days of neuronal differentiation, cell extracts were collected and performed by lysing cells with 250 µL of 0.01% (v/v) Triton X-100 in PBS (1 ×) followed by centrifugation at 16,000*g* for 5 min, at 4 °C.

Aminothiols in cell extracts and culture media (supernatants) were reduced with tris(2-carboxyethyl)phosphine (TCEP) derivatized with ammonium 7- fluoro-2,1,3-benzoxadiazole-4-sulfonate (SBD-F), as previously described by our group [48,49]. Samples were analysed by HPLC system (Shimadzu) with a RF-10AXL fluorescence detector, operating at 385 nm (λ excitation) and 515 nm (λ emission). The analytes Cys, CysGly, GluCys and GSH were separated on a LiChrospher 100 RP-18 (250 × 4 mm, 5 µm; Merck), with a mobile phase consisting of a mixture of 0.1 M acetate buffer (pH 4.5, adjusted with acetic acid): methanol (99:1 v/v), at a flow rate of 0.8 mL/min, at 29 °C. The run time was 20 min.

2.14. Statistical analysis

The data concerning cell culture were carried out at least in three independent preparations. Data are present as mean ± standard deviation (SD), n ≥ 3. Statistical comparisons between multiple groups were performed using one-way ANOVA. Whenever two groups were compared unpaired two-tailored *t*-test was used. In some specific cases, such as the analysis of western blot band intensity, Q-PCR for mRNA expression and Cys, CysGly, GluCys and GSH measurements, paired *t-tests* were performed. Statistical significance was considered for *p*-value bellow 0.05; *p*-values are described in the figures and the specific used analysis are described in figure's legends. Statistical analysis was performed in GraphPad Prism® Version 6.

3. Results

3.1. CORM-A1 increases neuronal differentiation yield

CORM-A1 modulatory effect on neuronal differentiation was assessed using SH-SY5Y cells, which have the ability to differentiate into neurons upon treatment with retinoic acid (RA) (Fig. 1A). CORM-A1 was used as a supplement of the classical differentiation procedure with RA. The neuronal differentiation process of SH-SY5Y cells occurs during 7 days, followed by 5 days of neuronal enrichment with anti-mitotic agent treatment (Fig. 1A).

After 7 days of differentiation, there is a mixed cell population composed of fully differentiated neurons and yet undifferentiated precursor cells [16]. This occurs mainly because cells are not synchronized in the beginning of the process. As expected, this population was composed of neurons and proliferative cells expressing Tuj1 and ki67 proteins, respectively, as assessed by immunocytochemistry (Fig. 1B). When SH-SY5Y cells were differentiated in the presence of 25 μM CORM-A1 supplementation, the total cell number of the mixed cell population at day 7 significantly increased, which was assessed by nuclei counting (Fig. 1C).

To further control that CORM-A1 effect is due to CO gas, CO-depleted inactive form iCORM-A1 was evaluated during neuronal differentiation. Neuronal differentiation triggered by RA and RA supplemented with iCORM-A1 presented the same amount of mixed cell population (Fig. S1). Thus, the observed increased levels of mixed cell population that follow neuronal differentiation with RA supplemented with CORM-A1 is dependent on CO gas.

In order to address whether this increase was due to an effect on cellular proliferation or differentiation, the mixed SH-SY5Y cell population was treated with anti-mitotic agents (for neuronal enrichment) for further neuronal cell quantification and morphology characterization by immunocytochemistry. Neuronal morphology is similar whenever differentiation was performed in the presence or absence of CORM-A1 (Fig. 1D). For the same amount of inoculated cells in the beginning of neuronal differentiation process, the enriched neuronal population increased about 4.5 times in the presence of CORM-A1 (Fig. 1E). Thus, CO released by CORM-A1 presents a positive modulatory role in neuronal differentiation of SH-SY5Y cell line. Moreover, it improves the final neuronal production yield, as also previously demonstrated in Almeida and co-authors (2016) [16].

3.2. CORM-A1 effect on glycolytic metabolism

Because neuronal differentiation involves modulation of glycolytic metabolism [2,3,50–52] and CO regulates cell metabolism [13,29], the CORM-A1 effect on glycolysis was assessed during neuronal differentiation. Characterization of cell metabolism, particularly the balance between glycolytic and oxidative metabolism, can be indirectly addressed by extracellular quantification of lactate production *per* glucose consumption over time [13]. When lactate production/glucose consumption ratio is 2 there might occur 100% of glycolysis. Also, as lower is this ratio, the higher is the level of oxidative phosphorylation. Herein lactate/glucose ratio remained unchanged with or without CORM-A1 supplementation during neuronal differentiation process (Fig. 2A); indicating that there might be no alteration on glycolysis or oxidative phosphorylation due to CO supplementation during SH-SY5Y neuronal differentiation.

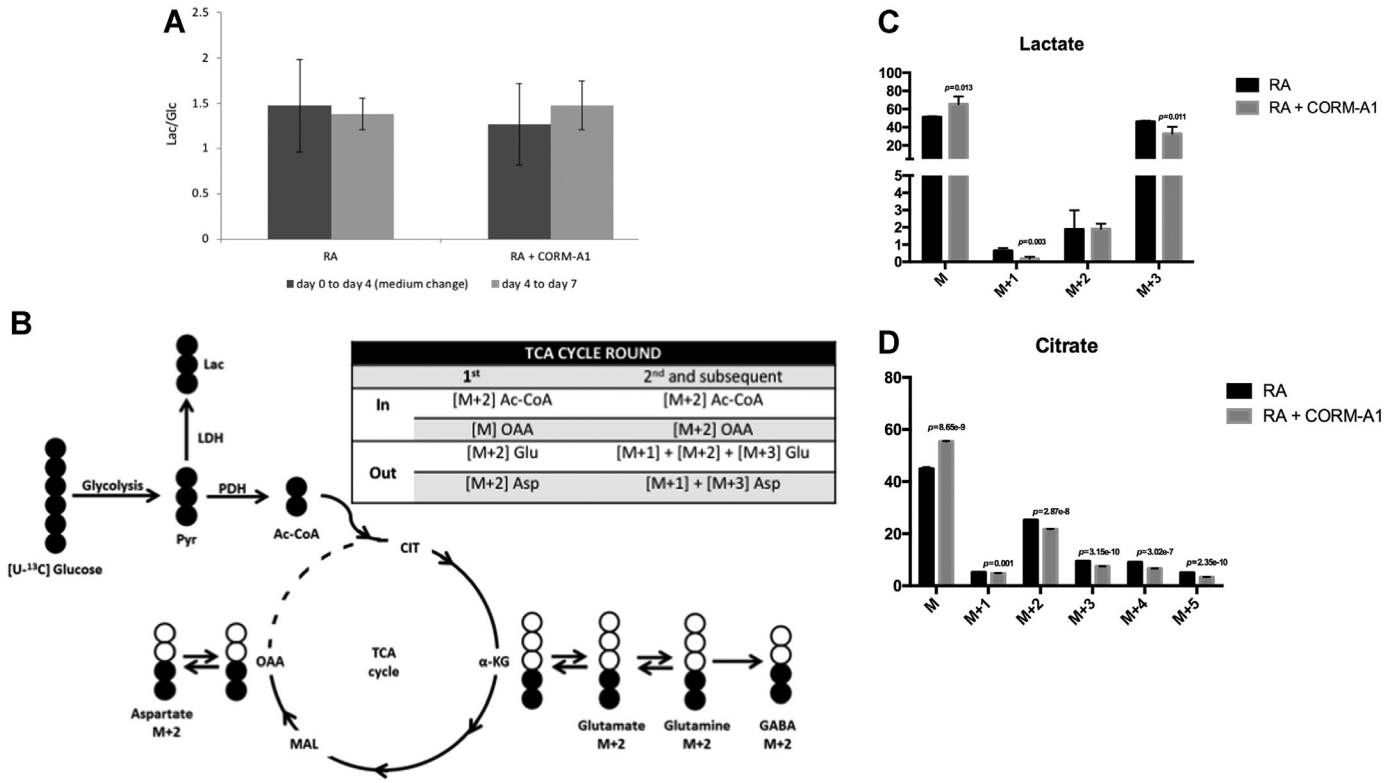

Fig. 2. Glycolytic metabolism profile. (A) Lactate production per glucose consumption (qLac/qGlc) ratios calculated between treatments: day 0 to day 4 and day 4 to day 7; (B) Labelling patterns derived from [U-^{13}C]glucose metabolism; The % enrichment with ^{13}C leading to the formation of molecules with masses: M + 1, M + 2 and M + 3 for (C) lactate, (D) citrate, (E) aspartate, (F) glutamine and (G) glutamate, determined by GC-MS analysis of SH-SY5Y cell extracts differentiated for 7 days and subjected to 24 h incubation with medium containing [U-^{13}C]glucose; dark grey corresponds to RA-treated cells and light grey to CORM-A1 supplemented cells, with *$p < 0.05$; (H) mRNA expression of specific metabolic markers (PDH for pyruvate dehydrogenase and LDH for lactate dehydrogenase) in SH-SY5Y mixed cell population after 7 days of neuronal differentiation. RPL22 was used as house-keeping gene and mRNA expression in non-differentiated cells was used as reference. The used statistical analysis was unpaired two-tailored *t-test*, while for panel H it was used paired *t-test*.

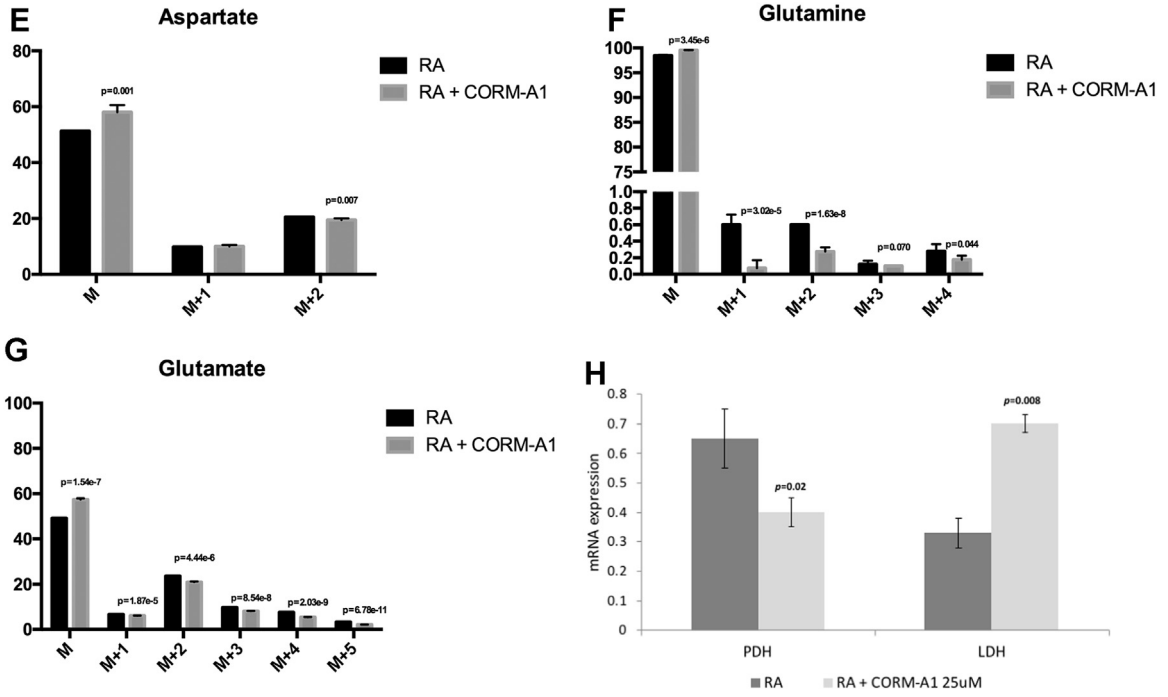

Fig. 2. (*continued*)

In order to further assess the role of glucose during neuronal differentiation, glycolysis flux progression was evaluated using labelled glucose (^{13}C) and GC-MS analysis. During glycolysis, glucose is converted in pyruvate, which can follow three distinct pathways: it can be converted (i) to lactate by lactate dehydrogenase (LDH) activity, (ii) to acetyl-CoA by pyruvate dehydrogenase (PDH) action followed by coenzyme A ligation, feeding the tricarboxylic acid cycle (TCA) or (iii) to alanine by reductive alkylation. To study ^{13}C enrichment in intracellular metabolites, SH-SY5Y cells differentiated for 7 days in the presence and absence of CORM-A1 supplementation were treated with [U-^{13}C] glucose for 24 h and cell extracts were prepared for GC-MS analysis. The percentage of ^{13}C enrichment was quantified in lactate, glutamine and glutamate, as well as in the TCA cycle metabolites citrate and aspartate. Metabolism of [U-^{13}C] glucose generates [U-^{13}C] lactate and [U-^{13}C] pyruvate. As shown in Fig. 2C, only about 50% of lactate incorporated ^{13}C, accordingly to the fact that differentiated neurons present low glycolytic levels. Moreover, neuronal metabolism relies mostly on oxidative phosphorylation and PPP is very active in neurons [17,53,54]. Nevertheless, there is a low difference of M + 3 lactate levels between control cells and CORM-A1 supplemented ones. These data corroborate the ratios of lactate production *per* glucose consumption presented in Fig. 2A, suggesting that there is no increase in glycolysis. In turn, [U-^{13}C] pyruvate is then converted into [1,2–^{13}C] acetyl CoA. This molecule condenses with non-labelled oxaloacetate to form double-labelled (M + 2) compounds in the first turn of the TCA cycle (Fig. 2B). Furthermore, in a combination of the first and second turn of the TCA cycle, [1,2–^{13}C] acetyl-CoA can condense with labelled oxaloacetate and give rise to the formation of diversely labelled compounds (Fig. 2B). GC-MS analysis of SH-SY5Y cell extracts treated with [U-^{13}C] glucose showed that the percentage of ^{13}C labelling of citrate, aspartate, glutamine and glutamate was decreased for M + 2 (Fig. 2D-G) in the presence of CORM-A1. In summary, CORM-A1 supplementation of SH-SY5Y cells during neuronal differentiation seems not to interfere with glycolysis, but it leads to a slight decrease in mitochondrial metabolism. Likewise, CORM-A1 supplementation promotes a decrease of mRNA expression of pyruvate dehydrogenase (PDH) and an increase on lactate dehydrogenase (LDH) mRNA expression (Fig. 2H). This result is in accordance with the lower mitochondrial metabolism observed in CORM-A1 supplemented cells (Fig. 2C-G) and with the unaltered ratio lactate/glucose and the amount of lactate obtained during differentiation in the presence of CORM-A1 (Fig. 2A and C, respectively). Consequently, one may hypothesize that, upon CORM-A1 supplementation, glucose can feed other pathways than glycolysis. PPP is a strong candidate pathway since it is important during cellular differentiation and it is parallel and interconnected to glycolysis. Likewise, PPP is a key cellular pathway against oxidative stress by increasing NADPH levels, which are needed for GSH/GSSG recycling. It is worthy of note that GSH is the first antioxidant cellular line of defence [8] and that GSH regeneration from GSSG is catalysed by glutathione oxidases and is dependent on electrons transferred from NADPH [55,56].

3.3. CORM-A1 modulates pentose phosphate pathway (PPP)

Our group has recently demonstrated that ROS are key signalling molecules in CO-induced SH-SY5Y neuronal differentiation because: (i) CO promoted anion superoxide and hydrogen peroxide production and (ii) N-acetylcysteine pre-treatment reverted CO-induced improvement of neuronal differentiation [16]. Thus, it can be hypothesized that CO-induced ROS production reinforces PPP in order to increase NADPH levels and to boost GSSG/GSH recycling system, which can limit potential oxidative stress. Therefore, PPP was indirectly addressed by GSH/GSSG ratio quantification. The GSH/GSSG ratio in cell extracts of neuronal differentiated SH-SY5Y cells with or without CORM-A1 supplementation was analysed by HPLC at the end of differentiation procedure day 7 (Fig. 3A). There is an increase of the intracellular GSH/GSSG ratio with CORM-A1 supplementation, which can be correlated with higher amounts of intracellular NADPH and consequently with PPP flux.

To further evaluate PPP during neuronal differentiation, mRNA expression of two PPP key enzymes was assessed, namely phosphogluconate dehydrogenase (PGDH) and transketolase (TKT), from oxidative and non-oxidative phases of PPP respectively (Fig. 3B). Actually, cellular expression of both enzymes increased in the presence of CORM-A1 during neuronal differentiation process (Fig. 3B). Likewise,

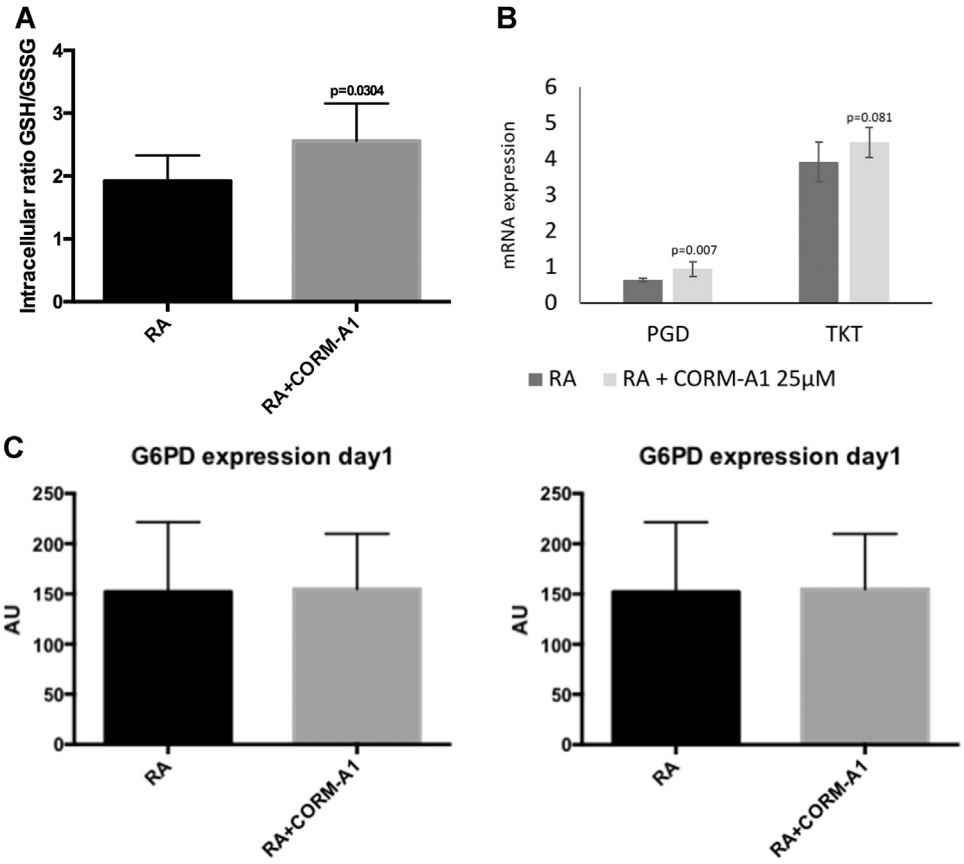

Fig. 3. CO modulation of pentose phosphate pathway. (A) GSH/GSSG ratios were obtained 7 days after CORM-A1 supplementation; unpaired *t-test* with * $p < 0.05$; (B) mRNA expression of specific PPP enzymes (PGDH for phosphogluconate dehydrogenase and TKT for transketolase) in SH-SY5Y mixed cell population after 7 days of neuronal differentiation. RPL22 was used as house keeping gene and mRNA expression in RA-treated cells was used as reference, with ** $p < 0.01$ and # $p < 0.1$; (C) Protein expression of G6PD after 24 h and 7 days of neuronal differentiation assessed by western blot, with # $p < 0.1$; (D) Quantification of enzymatic activity (mU/mg of protein) of G6PD in the presence of RA or RA + CORM-A1 after 7 days of neuronal differentiation. The used statistical analysis was paired two-tailored *t-test* for panels A, B and C, while for panel D it was used unpaired *t-test*.

protein expression level of the PPP rate-limiting enzyme glucose-6-phosphate dehydrogenase (G6PD) was quantified by western blot during neuronal differentiation process in the presence of CORM-A1 (Fig. 3C). After 24 h of neuronal differentiation, there is no difference in G6PD expression with CORM-A1 supplementation, while after 7 days an increase of G6PD expression is observed, although p-value is 0.0812, being above 0.05, which is usually the confidence interval for considering statistically different. (Fig. 3C). Furthermore, G6PD expression duplicates in SH-SY5Y cells treated with RA compared with non-treated cells (data not shown), indicating that PPP is a critical metabolic pathway in neuronal differentiation. Finally, G6PD activity was assessed following 7 days of neuronal differentiation and CORM-A1 supplementation increased G6PD enzymatic activity (Fig. 3D). In summary, the higher levels of PGDH and TKT mRNA and G6PD protein expression and activity in the presence of CORM-A1 supplementation, along with an increase in GSH/GSSG ratio, corroborate with the hypothesis of CO-induced PPP stimulation during neuronal differentiation.

3.4. Functional role of PPP during neuronal differentiation

In order to further validate the role of PPP during neuronal differentiation, G6PD was knocked down by small interference RNA (siRNA) approaches. By partially limiting PPP, one can validate its importance on neuronal differentiation process. Knocking down G6PD gene expression was confirmed by protein expression analysis via Western blot assay at 3 h and 24 h of neuronal differentiation (Supplementary Material Fig. S2). Whenever G6PD is knocked down, CO-induced increase on total cell population following 7 days of neuronal differentiation was reverted to similar levels as control cells treated only with RA (Fig. 4). Of note, no difference on total cell population was found in RA control with or without knocked down expression of G6PD, indicating that the role of PPP might be important only for the CO-induced improvement of neuronal differentiation. Thus, this data evidences that CO improvement on neuronal differentiation in SH-SY5Y cells is dependent on PPP stimulation.

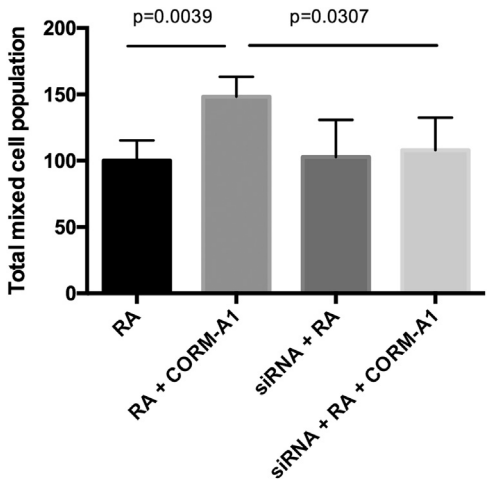

Fig. 4. Role of PPP during neuronal differentiation of SH-SY5Y cell line. Total mixed cell population, nuclei count *per* volume of SH-SY5Y cells and normalized by control cells treated with RA, following 7 days of differentiation, in the presence or absence of CORM-A1 supplementation and with down-regulation of G6PD expression. The used statistical analysis was unpaired two-tailored *t-test*.

3.5. CORM-A1 modulates glutathiolomic profile

The cell GSH/GSSG ratio is mostly dependent on GSH/GSSG recycling, which is associated with NADPH availability and PPP. Nevertheless, one might consider that the levels of GSH are also dependent on its synthesis and catabolism. Thus, it is also necessary to

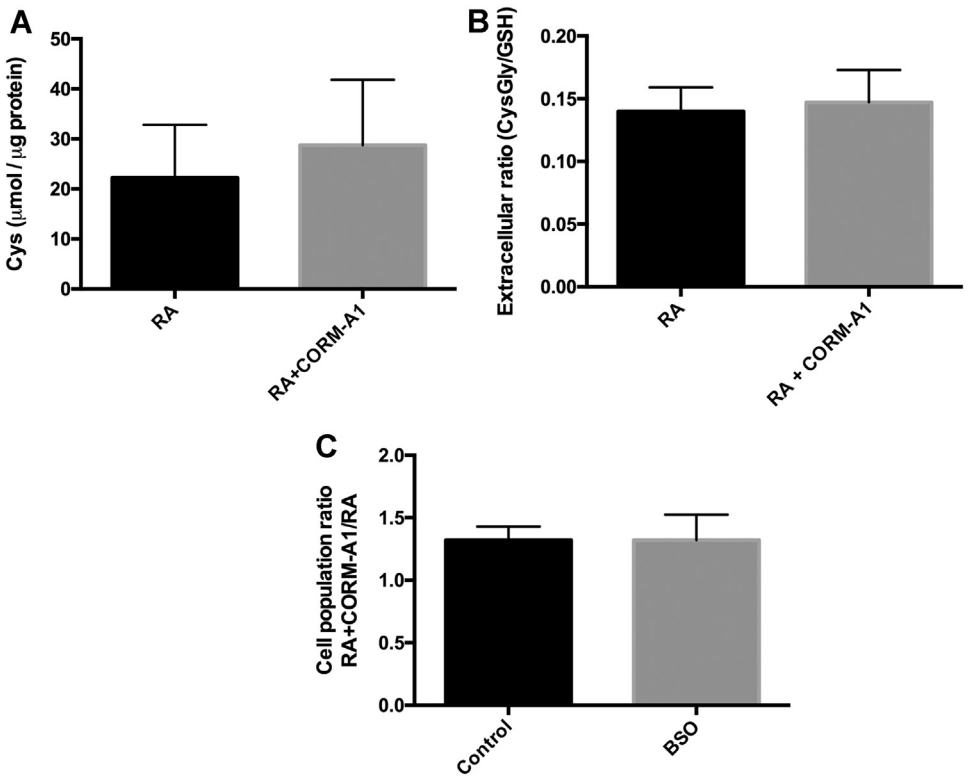

Fig. 5. CO modulation of glutathione metabolism. Following 7 days of neuronal differentiation in the presence and absence of CORM-A1 supplmentation, it was quantified (A) intracellular total cysteine; (B) extracellular ratio CysGly/GSH; (C) Total mixed cell population, nuclei count *per* volume of SH-SY5Y cells and normalized by control cells treated with RA, following 7 days of differentiation, in the presence of BSO for inhibiting GSH synthesis. Results are represented as the increase on total cell population due to CORM-A1 supplementation under control and BSO conditions.

evaluate the role of CO on glutathiolomic profile during neuronal differentiation. Quantification of intracellular precursors cysteine (Cys) and glutamyl-cysteine (GluCys) was used to address glutathione anabolism, being Cys the rate-limiting factor for GSH synthesis [57,58]. While evaluation of glutathione catabolism was performed by quantification of the ratio cysteinylglicine (CysGly) to glutathione in extracellular environment [58].

Cellular synthesis of glutathione is through the condensation of three aminoacids: cysteine, glutamate and glycine. CORM-A1 supplementation seems not to change glutathione anabolism, since intracellular levels of total cysteine are similar between control cells and cells treated with CORM-A1 during neuronal differentiation (Fig. 5A). Likewise, the levels of GluCys were below the detection limit of HPLC (0.625 μM) indicating that GSH synthesis occurs at residual levels or does not occur. Taken all together, these data might suggest that CO does not modulate GSH synthesis. Furthermore, no alteration in GSH catabolism was found, since the extracellular ratio of CysGly/GSH was not altered in the presence of CORM-A1 (Fig. 5B).

To further confirm that GSH synthesis does not play any role on the improvement of neuronal differentiation and the increase on GSH/GSSG ratio is due to PPP reinforcement, the role of CORM-A1 on neuronal differentiation was assessed in the presence of buthionine sulfoximine (BSO), which is a pharmacological inhibitor of GSH synthesis. Total mixed cell population at day 7 was counted and the growth on cell population was similar in the presence or absence of BSO (Fig. 5C). In conclusion, CORM-A1-induced improvement of neuronal differentiation is caused by an increase on PPP, promoting reduced GSH regeneration and is independent on new GSH synthesis or impaired catabolism.

4. Discussion

Our team has recently demonstrated that CO improves neuronal differentiation in a ROS dependent manner, using the human SH-SY5Y neuroblastoma cell line as a model [16]. Indeed, CO triggered ROS generation during neuronal differentiation, while N-acetylcysteine prevention of ROS production reverted the CO stimulation of neuronal differentiation [16]. The present work focuses on the role of CO in cell metabolism modulation, in particular the pentose phosphate pathway, since its metabolism is a key cellular process during neuronal differentiation [3].

CO reinforces oxidative phosphorylation and decreases glycolysis in several different models, namely astrocytes [13], carcinoma cells [59] or NT2 cells during neuronal differentiation [17]. Nevertheless, in the SH-SY5Y cell model of neuronal differentiation, CO supplementation did not change the balance between glycolysis and oxidative phosphorylation of SH-SY5Y cells during neuronal differentiation (Fig. 2). Therefore, the PPP was targeted as a potential metabolic pathway involved in CO's modulation of neuronal differentiation in the SH-SY5Y cell model. Although the PPP is a minor contributor to total glucose oxidation, it is essential for cellular function due to the importance of the products: (i) ribose-5-phosphate, which are building blocks for biosynthetic processes during neurogenesis and (ii) the electron donor NADPH that is needed for GSH recycling and antioxidant defence [60–65]. It is worthy of note that the GSH system is a key in antioxidant cell defence, by directly reacting with radicals and by being an electron donor in reactions catalysed by glutathione peroxidases, which in turn generates glutathione disulphide (GSSG) [8]. Thus, the CO-induced higher levels of ROS production during neuronal differentiation might promote the PPP stimulation in order to enhance the antioxidant defence through NADPH production and GSH recycling. In fact, CORM-A1 supplementation during SH-SY5Y cell line neuronal differentiation increased: (i) mRNA expression of 6-phosphogluconate dehydrogenase (PGDH) and transketolase (TKT) enzymes for oxidative and non-oxidative phases of PPP, respectively; (ii) protein expression and activity of glucose 6-phosphate dehydrogenase (G6PD) the rate-limiting enzyme of PPP and (iii) the intracellular ratio of GSH/GSSG (Fig. 3). Thus, one can conclude that CO does stimulate the PPP during neuronal differentiation in the SH-SY5Y cell line model. Likewise, whenever G6PD was knocked down using the siRNA approach and the PPP was partially inhibited, CO-induced improvement of neuronal differentiation reverted to levels similar to control, which is the standard RA treatment

(Fig. 4). Of note, modulation of PPP promoted endodermal differentiation of embryonic stem cells [66]. In conclusion, CO stimulates the PPP, which is already a well-established important metabolic pathway for neuronal differentiation.

In addition, PGDH and TKT are expressed in various cell types in the brain [67–69], but PGDH activity decreases after birth [70], while TKT activity increases during postnatal development [71,72]. Taking into account that there is low mRNA expression of PGDH and high mRNA expression of TKT, it can be speculated that SH-SY5Y cell model mimics adult neurogenesis. Moreover, in embryonic stem cells, it was observed that oxidative part of PPP was essential to generate NADPH to protect cells against oxidative stress but dispensable for the synthesis of ribose-5-phosphate (due to the interconnection to glycolysis) [73,74].

The cellular availability of reduced GSH is dependent on: GSSG reduction, GSH synthesis and GSH catabolism. The levels of total and free cysteine are similar in the presence or absence of CO, which indirectly indicates that CO does not modulate GSH synthesis. Likewise, the extracellular levels of CysGly/GSH ratio were found similar in the presence of CORM-A1, indicating no alteration on GSH catabolism. Finally, whenever GSH synthesis is pharmacologically inhibited by BSO, no CO-induced improvement was found on neuronal differentiation (Fig. 5). In conclusion, CO's improvement of neuronal differentiation is dependent on the increase of reduced GSH levels via metabolic regulation of PPP and enhanced generation of NADPH. Interestingly, Kaczara and colleagues have recently demonstrated that CORM-401 (a new CORM containing manganese as metal centre) enhances PPP in human endothelial cells [75].

Finally, in the present experiments CO did not affect glycolysis but slightly decreased mitochondrial metabolism (Fig. 3). These results are not in accordance with data previously published by our group [17], showing that CORM-A1 promotes neuronal differentiation of NT2 cells by reinforcing mitochondrial metabolism. In fact, the discrepancy between these results can be due to the different cell models used. NT2 are teratocarcinoma-derived cells that present a pluripotent phenotype, while SH-SY5Y cells already present a neuronal predisposition and have the ability to differentiate along the neuronal lineage. Thus, one can speculate that the NT2 cell line differentiation represents an early stage of neurogenesis process, while the SH-SY5Y cell line is a model more appropriate to characterize end phases of the neuronal differentiation process. Accordingly, at early stages, the switch from glycolytic to oxidative metabolism can be more relevant for the change between cell proliferation and the differentiation processes, which could explain the different CO effects in the NT2 and SH-SY5Y cell models.

In summary, our results (i) corroborate the importance of antioxidant defences during neuronal differentiation, (ii) present the PPP as relevant metabolic pathway for the modulation of neurogenesis and (iii) validate CO for improvement of neuronal yield by modulating the PPP and glutathione metabolism. Altogether, this study is a step forward in clarifying the role of cell metabolism involved in adult neurogenesis process.

Acknowledgements

This work was supported by the Portuguese Fundação para a Ciência e Tecnologia (FCT) grant FCT-ANR/NEU-NMC/0022/2012, FCT grant UID/Multi/04462/2013, I&D 2015-2020 iNOVA4Health - Programme in Translacional Medicine COST Action BM1005 “European Network on Gasotransmitters”, HLAV's FCT support IF/00185/2012, ASA's SFRH/BD/78440/2011 and NLS's PD/BD/127819/2016 fellowships.

Appendix A. Supplementary material

Supplementary data associated with this article can be found in the online version at http://dx.doi.org/10.1016/j.redox.2018.05.004.

References

[1] V.A. Rafalski, A. Brunet, Energy metabolism in adult neural stem cell fate, Prog. Neurobiol. 93 (2011) 182–203, http://dx.doi.org/10.1016/j.pneurobio.2010.10.007.
[2] V.A. Rafalski, E. Mancini, A. Brunet, Energy metabolism and energy-sensing pathways in mammalian embryonic and adult stem cell fate, J. Cell Sci. 125 (2012) 5597–5608, http://dx.doi.org/10.1242/jcs.114827.
[3] A.S. Almeida, H.L.A. Vieira, Role of cell metabolism and mitochondrial function during adult neurogenesis, Neurochem. Res. 42 (2017) 1787–1794, http://dx.doi.org/10.1007/s11064-016-2150-3.
[4] R. Dringen, H.H. Hoepken, T. Minich, C. Ruedig, Handbook of Neurochemistry and Molecular Neurobiology: Brain Energetics, in: A. Lajtha, G.E. Gibson, G.A. Dienel (Eds.), Integration of Molecular and Cellular Processes, Springer US, Boston, MA, 2007, pp. 41–62, , http://dx.doi.org/10.1007/978-0-387-30411-3_3.
[5] D.L. Nelson, M.M. Cox, Lehninger Principles of Biochemistry, 6th Editio, New York, 2013.
[6] A. Bilger, A. Nehlig, Quantitative histochemical changes in enzymes involved in energy metabolism in the rat brain during postnatal development. II. glucose-6-phosphate dehydrogenase and beta-hydroxybutyrate dehydrogenase, Int. J. Dev. Neurosci. 10 (1992) 143–152.
[7] H.L.A.H.L.A.A. Vieira, P.M.P.M. Alves, A. Vercelli, Modulation of neuronal stem cell differentiation by hypoxia and reactive oxygen species, Prog. Neurobiol. 93 (2011) 444–455, http://dx.doi.org/10.1016/j.pneurobio.2011.01.007.
[8] R. Dringen, Metabolism and functions of glutathione in brain, Prog. Neurobiol. 62 (2000) 649–671, http://dx.doi.org/10.1016/j.pneurobio.2014.01.002.
[9] S.W. Ryter, J. Alam, A.M. Choi, Heme oxygenase-1/carbon monoxide: from basic science to therapeutic applications, Physiol. Rev. 86 (2006) 583–650.
[10] I. Barbagallo, D. Tibullo, M. Di Rosa, C. Giallongo, G.A. Palumbo, G. Raciti, A. Campisi, A. Vanella, C.J. Green, R. Motterlini, A. Cytoprotective Role, for the heme oxygenase-1 / CO pathway during neural differentiation of human mesenchymal stem cells, J. Neurosci. Res. 86 (2008) 1927–1935, http://dx.doi.org/10.1002/jnr.21660.
[11] R. Gozzelino, V. Jeney, M.P. Soares, Mechanisms of cell protection by heme oxygenase-1, Annu. Rev. Pharmacol. Toxicol. 50 (2010) 323–354, http://dx.doi.org/10.1146/annurev.pharmtox.010909.105600.
[12] C.S.F. Queiroga, A.S. Almeida, C. Martel, C. Brenner, P.M. Alves, H.L.A. Vieira, Glutathionylation of adenine nucleotide translocase induced by carbon monoxide prevents mitochondrial membrane permeabilization and apoptosis, J. Biol. Chem. 285 (2010) 17077–17088, http://dx.doi.org/10.1074/jbc.M109.065052.
[13] A.S. Almeida, C.S.F. Queiroga, M.F.Q. Sousa, P.M. Alves, H.L.A. Vieira, Carbon monoxide modulates apoptosis by reinforcing oxidative metabolism in astrocytes, J. Biol. Chem. 287 (2012) 10761–10770, http://dx.doi.org/10.1074/jbc.M111.306738.
[14] N. Schallner, C.C. Romão, J. Biermann, W.A. Lagrèze, L.E. Otterbein, H. Buerkle, T. Loop, U. Goebel, Carbon monoxide abrogates ischemic insult to neuronal cells via the soluble guanylate Cyclase-cGMP pathway, PLoS One 8 (2013), http://dx.doi.org/10.1371/journal.pone.0060672.
[15] B. Wang, W. Cao, S. Biswal, S. Doré, Carbon monoxide-activated Nrf2 pathway leads to protection against permanent focal cerebral ischemia, Stroke 42 (2011) 2605–2610, http://dx.doi.org/10.1161/STROKEAHA.110.607101.
[16] A.S. Almeida, N.L. Soares, M. Vieira, J.B. Gramsbergen, H.L.A. Vieira, Carbon Monoxide Releasing Molecule-A1 (CORM-A1) improves neurogenesis: increase of neuronal differentiation yield by preventing cell death, PLoS One 11 (2016) e0154781, http://dx.doi.org/10.1371/journal.pone.0154781.
[17] A.S. Almeida, U. Sonnewald, P.M. Alves, H.L.A. Vieira, Carbon monoxide improves neuronal differentiation and yield by increasing the functioning and number of mitochondria, J. Neurochem. 138 (2016) 423–435, http://dx.doi.org/10.1111/jnc.13653.
[18] N. Dreyer-Andersen, A.S. Almeida, P. Jensen, M. Kamand, J. Okarmus, T. Rosenberg, S.D. Friis, A. Martínez Serrano, M. Blaabjerg, B.W. Kristensen, T. Skrydstrup, J.B. Gramsbergen, H.L.A. Vieira, M. Meyer, Intermittent, low dose carbon monoxide exposure enhances survival and dopaminergic differentiation of human neural stem cells, PLoS One 13 (2018) e0191207, http://dx.doi.org/10.1371/journal.pone.0191207.
[19] B.S. Zuckerbraun, B.Y. Chin, M. Bilban, J. de Costa d'Avila, J. Rao, T.R. Billiar, L.E. Otterbein, J.D.C. d'Avila, J. Rao, T.R. Billiar, L.E. Otterbein, Carbon monoxide signals via inhibition of cytochrome c oxidase and generation of mitochondrial reactive oxygen species, FASEB J. 21 (2007), http://dx.doi.org/10.1096/fj.06-6644com.
[20] H.S. Kim, P.A. Loughran, J. Rao, T.R. Billiar, B.S. Zuckerbraun, Carbon monoxide activates NF- B via ROS generation and Akt pathways to protect against cell death of hepatocytes, Am. J. Physiol. Gastrointest. Liver Physiol. 295 (2008) 146–152, http://dx.doi.org/10.1152/ajpgi.00105.2007.
[21] S. Lancel, S.M. Hassoun, R. Favory, B. Decoster, R. Motterlini, R. Neviere, Carbon monoxide rescues mice from lethal sepsis by supporting mitochondrial energetic metabolism and activating mitochondrial biogenesis, J. Pharmacol. Exp. Ther. 329 (2009) 641–648, http://dx.doi.org/10.1124/jpet.108.148049.could.
[22] H.B. Suliman, M.S. Carraway, L.G. Tatro, C. a Piantadosi, A new activating role for CO in cardiac mitochondrial biogenesis, J. Cell Sci. 120 (2007) 299–308, http://dx.doi.org/10.1242/jcs.03318.
[23] A.S. Almeida, C. Figueiredo-Pereira, H.L.A. Vieira, Carbon monoxide and mitochondriaâ€"modulation of cell metabolism, redox response and cell death, Front. Physiol. 6 (2015) 1–6, http://dx.doi.org/10.3389/fphys.2015.00033.
[24] H.B. Suliman, M.S. Carraway, A.S. Ali, C.M. Reynolds, K.E. Welty-wolf, C.A. Piantadosi, The CO / HO system reverses inhibition of mitochondrial biogenesis and prevents murine doxorubicin cardiomyopathy, J. Clin. Investig. 117 (2007) 3730–3741, http://dx.doi.org/10.1172/JCI32967.3730.
[25] M.A. Di Noia, S. Van Driesche, F. Palmieri, L.-M. Yang, S. Quan, A.I. Goodman, N.G. Abraham, Heme oxygenase-1 enhances renal mitochondrial transport carriers

and cytochrome C oxidase activity in experimental diabetes, J. Biol. Chem. 281 (2006) 15687–15693, http://dx.doi.org/10.1074/jbc.M510595200.
[26] R. Fukuda, H. Zhang, J.W. Kim, L. Shimoda, C.V. Dang, G.L. Semenza, HIF-1 regulates cytochrome oxidase subunits to optimize efficiency of respiration in hypoxic cells, Cell 129 (2007) 111–122, http://dx.doi.org/10.1016/j.cell.2007.01.047.
[27] C.S.F. Queiroga, A.S. Almeida, P.M. Alves, C. Brenner, H.L. a Vieira, Carbon monoxide prevents hepatic mitochondrial membrane permeabilization, BMC Cell Biol. 12 (2011) 10, http://dx.doi.org/10.1186/1471-2121-12-10.
[28] J. Shigezane, T. Kita, Y. Furuya, Acute and chronic effects of carbon monoxide on mitochondrial function, Igaku Kenkyu. 59 (1989) 35–45.
[29] K. AhlstrÖm, B. Biber, A. Åberg, A. WaldenstrÖm, G. Ronquist, P. Abrahamsson, P. StrandÉn, G. Johansson, M.F. Haney, Metabolic responses in ischemic myocardium after inhalation of carbon monoxide, Acta Anaesthesiol. Scand. 53 (2009) 1036–1042, http://dx.doi.org/10.1111/j.1399-6576.2009.01992.x.
[30] L. Lo Iacono, J. Boczkowski, R. Zini, I. Salouage, A. Berdeaux, R. Motterlini, D. Morin, A carbon monoxide-releasing molecule (CORM-3) uncouples mitochondrial respiration and modulates the production of reactive oxygen species, Free Radic. Biol. Med. 50 (2011) 1556–1564, http://dx.doi.org/10.1016/j.freeradbiomed.2011.02.033.
[31] R. Long, I. Salouage, A. Berdeaux, R. Motterlini, D. Morin, CORM-3, a water soluble CO-releasing molecule, uncouples mitochondrial respiration via interaction with the phosphate carrier, Biochim. Biophys. Acta - Bioenerg. 1837 (2014) 201–209, http://dx.doi.org/10.1016/j.bbabio.2013.10.002.
[32] C.S.F. Queiroga, A.S. Almeida, H.L.A. Vieira, Carbon monoxide targeting mitochondria, Biochem. Res. Int. 2012 (2012) 1–9, http://dx.doi.org/10.1155/2012/749845.
[33] S.R. Oliveira, C.S.F. Queiroga, H.L.A. Vieira, Mitochondria and carbon monoxide: cytoprotection and control of cell metabolism - a role for Ca 2+? J. Physiol. 594 (2016) 4131–4138, http://dx.doi.org/10.1113/JP270955.
[34] C.C. Romão, H.L.A. Vieira, Metal Carbonyl Prodrugs: CO Delivery and Beyond, (2015), http://dx.doi.org/10.1002/9783527673438.ch06.
[35] R. Motterlini, L.E. Otterbein, The therapeutic potential of carbon monoxide, Nat. Rev. Drug Discov. 9 (2010) 728–743, http://dx.doi.org/10.1038/nrd3228.
[36] R. Motterlini, P. Sawle, J. Hammad, S. Bains, R. Alberto, R. Foresti, C.J. Green, CORM-A1: a new pharmacologically active carbon monoxide-releasing molecule, Faseb J. 19 (2005) 284–286, http://dx.doi.org/10.1096/fj.04-2169fje.
[37] S. Pahlman, S. Mamaeva, G. Meyerson, M.E. Mattsson, C. Bjelfman, E. Ortoft, U. Hammerling, Human neuroblastoma cells in culture: a model for neuronal cell differentiation and function, Acta Physiol. Scand. Suppl. 592 (1990) 25–37.
[38] J. Kovalevich, D. Langford, Considerations for the Use of SH - SY5Y Neuroblastoma Cells in Neurobiology, in: Shohreh Amini, Martyn K White (Eds.), Neuronal Cell Cult. Methods Protoc. 2013, pp. 9–21, , http://dx.doi.org/10.1007/978-1-62703-640-5.
[39] R. Constantinescu, A.T. Constantinescu, H. Reichmann, B. Janetzky, Neuronal differentiation and long-term culture of the human neuroblastoma line SH-SY5Y, J. Neural Transm. Suppl. (2007) 17–28.
[40] J. Kovalevich, D. Langford, Considerations for the use of SH-SY5Y neuroblastoma cells in neurobiology, Methods Mol. Biol. 1078 (2013) 9–21, http://dx.doi.org/10.1007/978-1-62703-640-5_2.
[41] H. Xie, L. Hu, G. Li, SH-SY5Y human neuroblastoma cell line: in vitro cell model of dopaminergic neurons in Parkinson's disease, Chin. Med. J. 123 (2010) 1086–1092.
[42] S. Shavali, D.A. Sens, Synergistic neurotoxic effects of arsenic and dopamine in human dopaminergic neuroblastoma SH-SY5Y cells, Toxicol. Sci. 102 (2008) 254–261, http://dx.doi.org/10.1093/toxsci/kfm302.
[43] F.M. Lopes, R. Schröder, M.L.C. da Frota, A. Zanotto-Filho, C.B. Müller, A.S. Pires, R.T. Meurer, G.D. Colpo, D.P. Gelain, F. Kapczinski, J.C.F. Moreira, M.D.C. Fernandes, F. Klamt, Comparison between proliferative and neuron-like SH-SY5Y cells as an in vitro model for Parkinson disease studies, Brain Res. 1337 (2010) 85–94, http://dx.doi.org/10.1016/j.brainres.2010.03.102.
[44] L. Agholme, T. Lindstrom, K. Kagedal, J. Marcusson, M. Hallbeck, An in vitro model for neuroscience: differentiation of SH-SY5Y cells into cells with morphological and biochemical characteristics of mature neurons, J. Alzheimers Dis. 20 (2010) 1069–1082, http://dx.doi.org/10.3233/JAD-2010-091363.
[45] T.P. Mawhinney, R.S. Robinett, A. Atalay, M.A. Madson, Gas-liquid chromatography and mass spectral analysis of mono-, di- and tricarboxylates as their tert.-butyldimethylsilyl derivatives, J. Chromatogr. 361 (1986) 117–130.
[46] A.I. Amaral, M.G. Hadera, J.M. Tavares, M.R. Kotter, U. Sonnewald, Characterization of glucose-related metabolic pathways in differentiated rat oligodendrocyte lineage cells, Glia (2015), http://dx.doi.org/10.1002/glia.22900 (n/a-n/a).
[47] K. Biemann, The application of mass spectrometry in organic chemistry: determination of the structure of natural products, Angew. Chem. Int. Ed. Engl. 1 (1962) 98–111, http://dx.doi.org/10.1002/anie.196200981.
[48] T.D. Nolin, M.E. McMenamin, J. Himmelfarb, Simultaneous determination of total homocysteine, cysteine, cysteinylglycine, and glutathione in human plasma by high-performance liquid chromatography: application to studies of oxidative stress, J. Chromatogr. B Anal. Technol. Biomed. Life Sci. 852 (2007) 554–561, http://dx.doi.org/10.1016/j.jchromb.2007.02.024.
[49] N.M. Grilo, M. João Correia, J.P. Miranda, M. Cipriano, J. Serpa, M. Matilde Marques, E.C. Monteiro, A.M.M. Antunes, L.N. Diogo, S.A. Pereira, Unmasking efavirenz neurotoxicity: time matters to the underlying mechanisms, Eur. J. Pharm. Sci. 105 (2017) 47–54, http://dx.doi.org/10.1016/j.ejps.2017.05.010.
[50] J.-M. Kim, D. Jeong, H.K. Kang, S.Y. Jung, S.S. Kang, B.-M. Min, Osteoclast precursors display dynamic metabolic shifts toward accelerated glucose metabolism at an early stage of RANKL-stimulated osteoclast differentiation, Cell. Physiol. Biochem. 20 (2007) 935–946, http://dx.doi.org/10.1159/000110454.
[51] G. Pattappa, H.K. Heywood, J.D. de Bruijn, D.A. Lee, The metabolism of human mesenchymal stem cells during proliferation and differentiation, J. Cell. Physiol. 226 (2011) 2562–2570, http://dx.doi.org/10.1002/jcp.22605.
[52] B.T. Mischen, K.E. Follmar, K.E. Moyer, B. Buehrer, K.C. Olbrich, L.S. Levin, B. Klitzman, D. Erdmann, Metabolic and functional characterization of human adipose-derived stem cells in tissue engineering, Plast. Reconstr. Surg. 122 (2008) 725–738, http://dx.doi.org/10.1097/PRS.0b013e318180ec9f.
[53] P. Rodriguez-Rodriguez, E. Fernandez, J.P. Bolaños, Underestimation of the pentose–phosphate pathway in intact primary neurons as revealed by metabolic flux analysis, J. Cereb. Blood Flow Metab. 33 (2013) 1843–1845, http://dx.doi.org/10.1038/jcbfm.2013.168.
[54] X. Zheng, L. Boyer, M. Jin, J. Mertens, Y. Kim, L. Ma, L. Ma, M. Hamm, F.H. Gage, T. Hunter, Metabolic reprogramming during neuronal differentiation from aerobic glycolysis to neuronal oxidative phosphorylation, Elife 5 (2016), http://dx.doi.org/10.7554/eLife.13374.
[55] R. Dringen, H.H. Hoepken, T. Minich, C. Ruedig, 1.3 Pentose Phosphate Pathway and NADPH Metabolism, in: A. Lajtha, G.E. Gibson, G.A. Dienel (Eds.), Handb. Neurochem. Mol. Neurobiol. Brain Energ. Integr. Mol. Cell. Process. Springer US, Boston, MA, 2007, pp. 41–62, , http://dx.doi.org/10.1007/978-0-387-30411-3_3.
[56] J.M. Hansen, C. Harris, Glutathione during embryonic development, Biochim. Biophys. Acta 2015 (1850) 1527–1542, http://dx.doi.org/10.1016/j.bbagen.2014.12.001.
[57] A.P. Mazzetti, M.C. Fiorile, A. Primavera, M. Lo Bello, Glutathione transferases and neurodegenerative diseases, Neurochem. Int. 82 (2015), http://dx.doi.org/10.1016/j.neuint.2015.01.008.
[58] W.M. Johnson, A.L. Wilson-Delfosse, J.J. Mieyal, Dysregulation of glutathione homeostasis in neurodegenerative diseases, Nutrients 4 (2012) 1399–1440, http://dx.doi.org/10.3390/nu4101399.
[59] B. Wegiel, D. Gallo, E. Csizmadia, C. Harris, J. Belcher, G.M. Vercellotti, N. Penacho, P. Seth, V. Sukhatme, A. Ahmed, P.P. Pandolfi, L. Helczynski, A. Bjartell, J.L. Persson, L.E. Otterbein, Carbon monoxide expedites metabolic exhaustion to inhibit tumor growth, Cancer Res. 73 (2013) 7009–7021, http://dx.doi.org/10.1158/0008-5472.CAN-13-1075.
[60] O. Ben-Yoseph, P.A. Boxer, B.D. Ross, Noninvasive assessment of the relative roles of cerebral antioxidant enzymes by quantitation of pentose phosphate pathway activity, Neurochem. Res. 21 (1996) 1005–1012.
[61] O. Ben-Yoseph, P.A. Boxer, B.D. Ross, Oxidative stress in the central nervous system: monitoring the metabolic response using the pentose phosphate pathway, Dev. Neurosci. 16 (1994) 328–336.
[62] R. Dringen, B. Hamprecht, Involvement of glutathione peroxidase and catalase in the disposal of exogenous hydrogen peroxide by cultured astroglial cells, Brain Res. 759 (1997) 67–75.
[63] R. Dringen, L. Kussmaul, B. Hamprecht, Rapid clearance of tertiary butyl hydroperoxide by cultured astroglial cells via oxidation of glutathione, Glia 23 (1998) 139–145.
[64] L. Kussmaul, B. Hamprecht, R. Dringen, The detoxification of cumene hydroperoxide by the glutathione system of cultured astroglial cells hinges on hexose availability for the regeneration of NADPH, J. Neurochem. 73 (1999) 1246–1253.
[65] B. Rahman, L. Kussmaul, B. Hamprecht, R. Dringen, Glycogen is mobilized during the disposal of peroxides by cultured astroglial cells from rat brain, Neurosci. Lett. 290 (2000) 169–172.
[66] G. Manganelli, A. Fico, U. Masullo, F. Pizzolongo, A. Cimmino, S. Filosa, Modulation of the pentose phosphate pathway induces endodermal differentiation in embryonic stem cells, PLoS One 7 (2012) e29321, http://dx.doi.org/10.1371/journal.pone.0029321.
[67] R.S.J. Rust, J.G. Carter, D. Martin, J.M. Nerbonne, P.A. Lampe, M.E. Pusateri, O.H. Lowry, Enzyme levels in cultured astrocytes, oligodendrocytes and Schwann cells, and neurons from the cerebral cortex and superior cervical ganglia of the rat, Neurochem. Res. 16 (1991) 991–999.
[68] F.C. Kauffman, The quantitative histochemistry of enzymes of the pentose phosphate pathway in the central nervous system of the rat, J. Neurochem. 19 (1972) 1–9.
[69] N.Y. Calingasan, K.F. Sheu, H. Baker, E.H. Jung, F. Paoletti, G.E. Gibson, Heterogeneous expression of transketolase in rat brain, J. Neurochem. 64 (1995) 1034–1044.
[70] G. Bagdasarian, D. Hulanicka, Changes of mitochondrial glucose-6-phosphate dehydrogenase and 6-phosphogluconate dehydrogenase during brain development, Biochim. Biophys. Acta 99 (1965) 367–369.
[71] N.Z. Baquer, J.S. Hothersall, P. McLean, A.L. Greenbaum, Aspects of carbohydrate metabolism in developing brain, Dev. Med. Child Neurol. 19 (1977) 81–104.
[72] H. Iwata, H. Tonomura, T. Matsuda, Transketolase and 2-oxoglutarate dehydrogenase activities in the brain and liver of the developing rat, Experientia 44 (1988) 780–781.
[73] P.P. Pandolfi, F. Sonati, R. Rivi, P. Mason, F. Grosveld, L. Luzzatto, Targeted disruption of the housekeeping gene encoding glucose 6-phosphate dehydrogenase (G6PD): G6PD is dispensable for pentose synthesis but essential for defense against oxidative stress, EMBO J. 14 (1995) 5209–5215.
[74] S. Filosa, A. Fico, F. Paglialunga, M. Balestrieri, A. Crooke, P. Verde, P. Abrescia, J.M. Bautista, G. Martini, Failure to increase glucose consumption through the pentose-phosphate pathway results in the death of glucose-6-phosphate dehydrogenase gene-deleted mouse embryonic stem cells subjected to oxidative stress, Biochem. J. 370 (2003) 935–943, http://dx.doi.org/10.1042/BJ20021614.
[75] P. Kaczara, B. Proniewski, C. Lovejoy, K. Kus, R. Motterlini, A.Y. Abramov, S. Chlopicki, CORM-401 induces calcium signalling, NO increase and activation of pentose phosphate pathway in endothelial cells, FEBS J. (2018), http://dx.doi.org/10.1111/febs.14411.